The Utilization of Statistical Properties of Satellite-Derived Atmospheric Motion Vectors to Derive Quality Indicators

KENNETH HOLMLUND

European Organisation for Meteorological Satellites, Darmstadt, Germany

(Manuscript received 5 December 1997, in final form 22 April 1998)

ABSTRACT

The extraction of atmospheric motion vectors (AMVs) from cloud and moisture features from successive geostationary satellite images is an established and important data source for numerical weather prediction (NWP). So far the extraction of AMVs has been confined to the main synoptic times only, which grossly underutilizes the potential of these satellite-derived data. The advent of four-dimensional variational assimilation techniques provides the opportunity to utilize data derived at asynoptic times. This will enhance the capabilities of geostationary satellite systems that can provide continuous and near–real time observations. The new assimilation schemes are able to digest data representing various scales and with variable quality, which further enhances the usefulness of the satellite data. In order to fully exploit the AMVs derived with satellite data, it is imperative to accurately assess the quality and representativeness of individual wind vectors and to provide this information to the NWP centers as an integral part of the observations in near real time. The required high production and dissemination frequency cannot be met if manual intervention is required; hence, the emphasis has to be on fully automated schemes. This paper will describe the automatic quality control scheme implemented at EUMETSAT. It is based on the statistical properties of the derived AMVs and it provides a quality indicator (QI), describing the expected quality of every individual vector. The derived QIs are currently disseminated together with the derived vectors. The paper will also provide validation results based on collocated radiosonde statistics and report on first experiences by ECMWF in utilizing the QIs.

1. Introduction

The operational production of wind vector fields in the troposphere from satellite observations is currently confined to data from the geostationary satellites, namely Meteosat [European Organisation for Meteorological Satellites (EUMETSAT)], GOES [National Oceanic and Atmospheric Administration/National Environmental Satellite, Data and Information System (NOAA/NESDIS) in the United States], GMS [Japanese Meteorological Agency (JMA)], and Insat (Indian Meteorological Department, India) (e.g., CGMS XXIII 1995). During the past few years the instrumentation on board these spacecraft has improved, particularly on GOES (Geostationary Operational Environmental Satellite) and GMS (Geostationary Meteorological Satellite), providing extended capabilities for the wind derivation process. Already vector fields are derived not only with images from the infrared window channels, but also from the visible and water vapor channels. This provides the capability to track not only cloud targets but also water vapor features (e.g., Nieman et al. 1997; Velden et al. 1997; Bhatia et al. 1996; Tokuno 1996; Rattenborg and Holmlund 1996). These atmospheric motion vector (AMV) fields are presently scrutinized at several data production centers with stringent automatic and in some cases also with manual quality control (QC). The goal of the QC is to extract those vectors that display an accuracy similar to radiosonde (R/S) measurements. The need to do so is due to the fact that currently the AMVs are mainly utilized in the data assimilation for numerical weather prediction (NWP) as single-level point measurements. The continuous improvements in the instrumentation, the extraction schemes, and the successful implementation of the QC concepts are confirmed by the increasing role these vector fields have, not only in the data assimilation for global NWP, especially over the data-void ocean areas (e.g., Kelly 1993; Thoss 1992), but also for the prediction of severe weather phenomena (e.g., Velden et al. 1992; Velden 1996). Many of the current operational QC procedures are quite stringent and remove a large fraction of vectors from the final product; for example, at EUMETSAT, only about 20% of the derived vectors are currently disseminated operationally.

The introduction of new assimilation schemes, for example, four-dimensional variational schemes, enables the use of data with variable quality and data derived

Corresponding author address: Kenneth Holmlund, EUMETSAT, Am Kavalleriesand 31, 64295 Darmstadt, Germany.
E-mail: holmlund@eumetsat.de

at asynoptic times (e.g., Tsuyuki 1996; Thépaut et al. 1993). This, in conjunction with the anticipated reduction in ground-based upper-air observation systems, emphasizes the potential value of the geostationary observation systems. These systems can provide global coverage at a frequency related to the image repeat cycle, which for the present systems is 30 min or better. In order to increase the current AMV extraction frequency and coverage, the traditional quality control schemes have to be reconsidered as the amount of disseminated vectors will be greatly increased as compared to previous years. It will no longer be practical to involve manual quality control and only fully automated schemes are desirable. Nieman et al. (1997) report that the manual quality control has already been completely abandoned at NOAA/NESDIS and at EUMETSAT efforts are also concentrated on improving the automatic quality control (AQC) procedures. These new methods are deriving quality flags for individual vectors, which are used to filter out vectors with gross errors.

A successful AQC scheme would not supply simple flags for every individual vector, but would retain information on the reliability of the tracking, the accuracy of the height assignment, and the representative scale of the derived vectors. This would enable a higher dissemination frequency and better coverage, as potentially useful vectors would not be removed by the quality control scheme. The task of the data provider would then be to remove vectors with gross errors. Typically these very poor vectors are related to problems in the correlation procedures deriving the displacements or to the determination of the height of the vectors and to orographic effects. The final use of the vectors would then be controlled by the end user to best suit his application. In NWP the variable quality indicators (QIs) could be used to modify the error characteristics used in the models for the particular observations. Hence vectors representing scales and motions well suited for assimilation would get a larger impact than vectors that represent scales and motions that are not well described in the models.

2. The derivation of quality flags

a. Background

At midlatitudes the geostrophic approximation can be used to determine the flow of large-scale motion (e.g., Holton 1979). Geostrophic balance only occurs when there is no curvature of the flow. Taking the curvature into account, one can define the gradient flow in a frictionless environment. The gradient flow is a three-way balance between the Coriolis force, the centrifugal force, and the horizontal pressure gradient force. It can be shown that the ratio of the geostrophic wind to the gradient wind (V_g/V) is

$$V_g/V = 1 + R, \tag{1}$$

where R is the Rossby number (Holton 1979).

From the above formulation we see that at midlatitudes, where $R = 0.1$ for typical synoptic scales of the order of 1000 km, the geostrophic approximation deviates from the gradient in the order of 10%. Another error in the geostrophic approximation originates from neglecting the acceleration term (dV/dt) in the horizontal momentum equations, which generally is a magnitude of order smaller than the main terms. Following the above argument it can be expected that any deviations in flow should be within 10%–20% of a continuous straight flow in the free atmosphere. Tracking a passive tracer in the atmosphere over limited and consecutive periods of time should therefore provide displacement vectors that are highly similar in direction and magnitude. It should be noted that for smaller-scale motion or close to the surface as well as at low latitudes, where the geostrophic approximation becomes invalid, larger deviations than described above can occur. Also within jet stream areas, strong ageostrophic winds can be observed. Prater (1996) used an aircraft flown along an isentropic surface to make in situ measurements and to follow a drifting pointer. In a polar jet stream exit area he found large decelerations on the order of 5 m s^{-1} during time periods of roughly 2000 s, which is of the same timescale as the observation frequency (30-min cycle) used in many AMV extraction schemes. In this case the original wind speed was close to 40 m s^{-1}, so the deceleration was roughly 12%. The total estimated ageostrophic wind was between 6.6 and 23.1 m s^{-1}, that is, up to 57% of the initial wind speed.

The target selection methods applied in the wind derivation schemes at EUMETSAT attempt to extract tracers that are stable in time. It can therefore be expected that two AMVs derived from a consecutive image triplet should show a high degree of agreement in speed and direction. This basic knowledge has been used in the most common AQC tests, namely, the speed, direction, and vector symmetry tests. These tests are successfully used as a basis for the traditional AQC at several centers deriving winds from satellite data (e.g., Le Marshall et al. 1994; Tokuno 1996; Bhatia et al. 1996) but similar methods are also applied to ground-based observations (DeGaetano 1997).

A quality check of consecutive vector pairs should reject erroneous accelerations but allow for natural accelerations in, for example, jet entrance–exit regions. At the European Space Operations Centre (ESOC) the speed symmetry test was empirically tuned to extract the best fraction of winds describing the large-scale flow. The maximum allowed acceleration for two consecutive vectors was set to 50% of the mean wind speed (Nuret 1990), which agrees well with the above observations. Also the other satellite operators have used thresholds of the same order of magnitude. For example, at JMA (Tokuno 1996) the maximum allowed speed difference for high-level winds is set to 10 m s^{-1} for average wind speeds between 20 and 25 m s^{-1}.

In a similar fashion to the consistency in time, the

horizontal consistency of the derived vectors can be used to identify poor vectors. Endlich and McLean (1957) found that over latitude bands of 1° (ca. 110 km) the jet core wind speed can typically decrease about 15%. The typical target size is at many extraction centers of the order of 100–200 km per side for a square target. A test, which compares the extracted vectors to their surrounding vectors, should therefore take this potential variability into account. At ESOC this so-called local consistency check (Holmlund 1994) compared every extracted vector with a speed greater than 15 m s^{-1} to the maximum eight surrounding vectors with a maximum height difference of 30 hPa. The maximum allowed speed difference was 3 m s^{-1}, which is 10%–15% of the typical high-level wind speeds.

Furthermore, a test against the forecast vector interpolated to the location of the derived displacement vector is often included. This last test can be quite problematic, as a very stringent application of this test would only reproduce the forecast field. In such a scheme manual intervention has proven important to assure that no significant true deviations from the forecast field would be filtered out. The generally applied thresholds are of the same magnitude of order as the symmetry checks.

b. Quality indicators

The fact that the real ageostrophic wind components can vary significantly from case to case indicates that the simple application of thresholds can either remove potentially valuable vectors or it may not be tight enough such that poor vectors remain accepted. The use of manual quality control to ascertain that these winds can be accepted is not practical for large amounts of data. To meet this challenge the recursive filter (RF) objective analysis was developed at NOAA/NESDIS (Hayden and Purser 1995). It attempts to retain as much as possible of the preexisting information by automatically adjusting the derived components to be internally coherent and consistent with existing background fields. The RF has proven to be successful on a synoptic scale (Hayden and Velden 1991; Menzel et al. 1996). Also, in cases where the background field is poor the RF is capable of maintaining the correct flow pattern provided a sufficiently large number of consistent observations is available. Velden (1996) showed a significant improvement in tropical storm tracking with water vapor wind vector (WVWV) fields controlled with a tuned RF quality control system. Additional details on the RF and its applications to AMVs can be found in Velden et al. (1998).

An alternative method is to estimate the reliability of the derived vectors based on several quality control tests, which are based on the information in the derived vector field itself. A large number of tests were validated for quality control purposes at ESOC (Holmlund 1995). The tests were based on consistency checks in space and time, not only for the vector components, but also for the height and temperature of the tracer. Furthermore, a test based on the variability of the measured radiance within the target area as well as a test related to the presence of multilayered cloud scenes were included. Many of the applied tests were similar to the tests involved in the traditional approach, but instead of rejecting vectors showing large deviations in any of its components, only the probability of the vector being poor was increased.

During a two-week period in August–September 1994, WVWVs were produced and disseminated on a half-hourly basis to the European Centre for Medium-Range Forecasts (ECMWF), providing comparisons against the ECMWF first-guess and background fields (CGMS XXIII 1995). The importance of the individual tests as well as the different combination of tests were estimated by comparing the derived quality marks to the mean vector difference between the WVWVs and the ECMWF first-guess wind field. Furthermore, experienced shift meteorologists were visually verifying the performance of the different tests for selected cases. This was quite important to avoid misinterpretation of the results in, for example, jet stream areas, where the global analyses and forecasts of peak winds are still systematically too weak (e.g., Tenenbaum 1996). The most suitable tests were related either to the symmetry of the vector pair, which is achieved by tracking the targets in at least three consecutive images, and/or differences to the surrounding vectors. It should be noted that these investigations confirmed the necessity of applying several tests, as no single test was able to remove all poor vectors and the best agreement with the ECMWF first guess was achieved by combining several tests.

Based on the previous experiences, a set of tests was selected and further tuned for the operational extraction of QIs at EUMETSAT. In the new approach a forecast test is also included. The forecast test is based on the vector difference between the forecast (usually a 12- or 18-h forecast) and the derived AMV, but even vectors with a large difference from the forecast are not necessarily excluded from dissemination, providing that the other tests turn out well. Therefore the dependency on the forecast in the new AQC scheme is reduced as compared to a thresholding scheme.

Currently five tests are included in the EUMETSAT AQC scheme. Table 1 presents the tests and the test functions, where $D_i(x, y)$, $V_i(x, y)$, and $\mathbf{S}_i(x, y)$ are the direction, speed, and vector derived from the first image pair ($i = 1$) or the second image pair ($i = 2$) of an image triplet at location (x, y). Here, $\mathbf{S}(x, y) = \mathbf{S}_1(x, y) + \mathbf{S}_2(x, y)$ and $\mathbf{F}(x, y)$ is the interpolated forecast vector; $\mathbf{S}(x - i, y - j)$ refers to the vectors in the surrounding locations in the EUMETSAT segment coordinates (Bühler and Holmlund 1994). The spatial test is only applied to vectors within a predefined pressure range (currently 100 hPa) centered at the height of the central vector $[\mathbf{S}(x, y)]$. This test therefore also includes a height

TABLE 1. The EUMETSAT AMV consistency tests.

Test name	Function
Direction	$\lvert D_2(x, y) - D_1(x, y)\rvert / \langle 20 \exp^{-\{[V_2(x, y) + V_1(x, y)]/20\} + 10} \rangle$
Speed	$\lvert V_2(x, y) - V_1(x, y)\rvert / \{0.1 [V_2(x, y) + V_1(x, y)] + 1\}$
Vector	$\lvert \mathbf{S}_2(x, y) - \mathbf{S}_1(x, y)\rvert / \{0.1 [\lvert \mathbf{S}_2 (x, y) + \mathbf{S}_1 (x, y)\rvert] + 1\}$
Spatial	$\lvert \mathbf{S} (x, y) - \mathbf{S} (x - i, y - j)\rvert / \{0.1 [\lvert \mathbf{S}(x, y) + \mathbf{S}(x - i, y - j)\rvert] + 1\}$
Forecast	$\lvert \mathbf{S}(x, y) - \mathbf{F}(x, y)\rvert / \{0.2 [\lvert \mathbf{S}(x, y) + \mathbf{F}(x, y)\rvert] + 1\}$

consistency check, and if no surrounding vectors are found within this pressure range, the test will return the value 0 (indicating a poor quality). The test provides only a rough estimate on the consistency of the height assignment with respect to the surroundings and does not attempt to estimate the absolute error of the assigned height.

It should be noted that it is assumed that the errors are symmetrical; for example, the vectors are equally poor if they have a directional difference of $+30°$ and $-30°$. The selected tests are to a large extent independent; only the vector test shows similar behavior to two other tests, namely, the speed test and the direction test. The speed dependency in the direction test is, in order to better identify misaligned tracking, different from that of the vector test and therefore the use of a separate vector test is justified.

The combination of the results to provide one estimate on the reliability of the vectors was successfully demonstrated during a two-week period in 1994 (CGMS XXIII 1995) during which a combined QI for WVWVs was validated against the ECMWF first guess. The selected approach at EUMETSAT has therefore been to combine the individual test results to a final quality indicator.

c. Normalized quality indicators

In order to combine the results from the individual tests, the test results have to be normalized into a specific range. The distributions of wind speed and direction have been investigated extensively for climatological and statistical purposes (e.g., Berz 1983). The distributions are often non-Gaussian, and therefore it is reasonable to assume that the distributions of the tests applied in the AQC will also have non-Gaussian distributions. Of more interest than the actual distribution is the cumulative distribution function (CDF) $\Phi(t)$, which for a distribution function $f(x)$ is defined by

$$\Phi(t) = \int_{-\infty}^{t} f(x)\, dx. \tag{2}$$

Figure 1 presents the cumulative distribution of all tests as specified in Table 1.

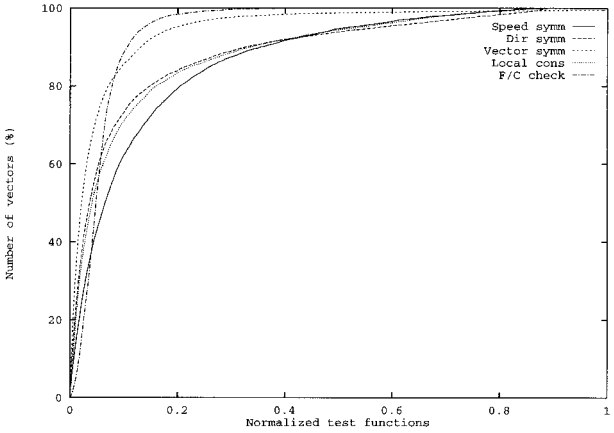

FIG. 1. The CDF of all tests applied operationally at EUMETSAT.

The general behavior is similar for all tests. It should be noted that, as explained in section 2a, it can be expected that due to meteorological conditions a deviation from a test value of zero does not automatically indicate that the vector in question would have a deteriorated quality. This can be illustrated by, for example, the direction test, where a small deviation in direction can be related to curvature of the flow and not to poor tracking or to a changing target. These small deviations should also be accounted for in the normalization, which therefore is currently performed with a simple tanh-based function instead of the true CDF:

$$\Phi_i(x) = 1 - \{\tanh[f_i(x)]\}^{a_i}. \tag{3}$$

The advantage of this function is that small deviation from the zero value can easily be set to return values close to one (representing high quality) and any test value will return a quality between zero and one. Figure 2 shows the behavior $\Phi_i(x)$ for currently used values of a_i ($a_i = 2$ for F/C test, $a_i = 4$ for direction test, and $a_i = 3$ for the other tests).

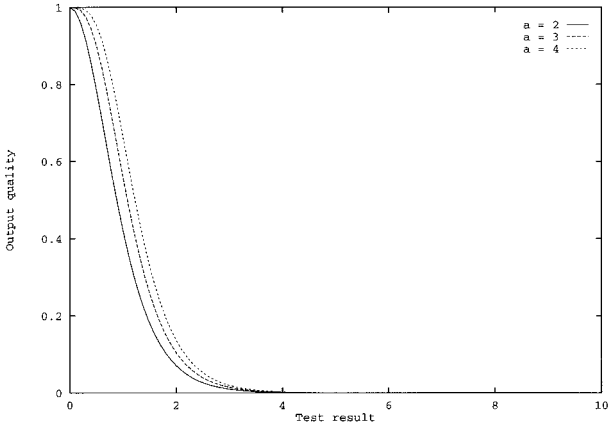

FIG. 2. The behavior of the normalization function $\Phi_i(x)$ for different values of a_i.

After normalization the tests deliver normalized quality indicator (NQI) values, which have a similar distribution; that is, a vector with a good test results will have an NQI close to one, whereas a poor result will return a value close to zero. The final QI of the vectors is defined as the weighted average of the NQI delivered by $\Phi_i(x)$:

$$\mathrm{QI} = \left[1\Big/\left(\sum w_i\right)\right] \sum w_i \Phi_i(x), \tag{4}$$

where w_i is a test-dependent weight. In parallel to the tuning of the test parameters, the weights of the individual tests were tuned by decomposing the impact of the individual tests. Several case studies indicated that all tests should have the same weight, except for the spatial consistency test that should have a double weight. This setup has been selected as the operational configuration.

3. Verification of the results

a. Subjective analysis of a typical case

The performance of the AQC can be subjectively evaluated by inspecting images together with the vector fields and their assigned quality. Figure 3 presents the wind vector field on 7 March 1996, derived from consecutive water vapor images.

The four vector fields represent a subsection of the complete vector field derived over the same area over the South Atlantic region, filtered with QI, such that the presented vectors have a quality higher than the applied threshold value. The applied threshold for the upper-left image is 0.0 (i.e., all vectors are displayed); for the bottom left, 0.2; and for the bottom right, 0.7. As a comparison the vectors accepted by the traditional AQC are presented in the top-right picture.

During the traditional AQC, a wind vector failing at least one of the applied quality tests was rejected. This approach, applied, for example, at the Meteorological Information Extraction Centre at ESOC/ESA (European Space Agency) until the end of 1995 (Schmetz et al. 1993), rejected the major part of the vector field, including some vectors that were potentially good. After the AQC a manual check was performed, during which further poor vectors could be removed or potentially valuable vectors reinstated.

The total number of vectors derived over the full Meteosat field of view was 3374. It is informative to mention that the old approach, however, without manual intervention, accepted 17% of the vectors. The presented section shows a vector field with a high degree of consistency with the forecast field described by the streamlines at 300 hPa. The 0.2 QI threshold accepts 82% of the vectors and in this subsection all apparently poor vectors are removed.

The QI level 0.7 accepts 37% of the original vectors, which is roughly twice the amount of the conservative thresholding applied in the traditional AQC. In the presented section some further vectors not fully consistent with the general pattern are removed as compared to the picture related to the QI level 0.2. It should also be noted that a lot of vectors deviating from the forecast field are still surviving the AQC. These vectors, that is, mainly in the upper part of the subsection, are related to the trough in the top-right area and to the wave disturbance in the middle and seem realistic taking the image data into account.

The subjective analysis indicates that the quality control is performing as expected, but in order to manifest this observation an objective analysis of the vector fields is also required.

b. Validation against collocated R/S measurements

To achieve a reliable estimate of the quality of the vectors a reference dataset is required. At the moment the AMVs are mainly used as single-point measurements equivalent to radiosonde measurements. It is therefore natural to use the radiosonde data for verification purposes. It is, however, important to recognize that the radiosonde measurements also contain errors and do not provide an absolute truth. Using long-term statistics it is possible to show that the vector difference rms error ($\mathrm{dvec_{rms}}$) between the satellite-observed and radiosonde measurements is linearly dependent on the wind speed as measured by the radiosonde ($|\mathrm{vec_{R/S}}|$) (Schmetz et al. 1993; Velden et al. 1997). The slope of the relationship can then be defined by

$$\mathrm{A} = (\mathrm{dvec_{RMS}} - \mathrm{B})/|\mathrm{vec_{R/S}}|. \tag{5}$$

The coefficients (A and B) can be derived during periods with no interventions in the extraction scheme. During periods with frequent changes in the algorithms used in the product extraction it is not possible to accurately define A and B. In order to be able to compare different periods, we define the normalized vector difference rms (Nrms) error as

$$\mathrm{Nrms} = \mathrm{dvec_{rms}}/|\mathrm{vec_{R/S}}|. \tag{6}$$

Using Nrms it is possible to get a rough indication of the performance of the system without knowing A and B. Comparing the Nrms for two subperiods (1 and 2) of a period with constant coefficients A and B using 5, we get

$$[\mathrm{dvec_{rms}}(1) - \mathrm{B}]/|\mathrm{vec_{R/S}}(1)| = [\mathrm{dvec_{rms}}(2) - \mathrm{B}]/|\mathrm{vec_{R/S}}(2)|, \tag{7}$$

where (1) and (2) refer to the two subperiods. After rearranging and substituting with (6) we have

$$\Delta\mathrm{Nrms} = \mathrm{Nrms}(1) - \mathrm{Nrms}(2) = \mathrm{B}/|\mathrm{vec_{R/S}}(1)| - \mathrm{B}/|\mathrm{vec_{R/S}}(2)|. \tag{8}$$

In this case ΔNrms should, as A and B are constant, be close to zero and not equal to $[\mathrm{B}/|\mathrm{vec_{R/S}}(1)| -$

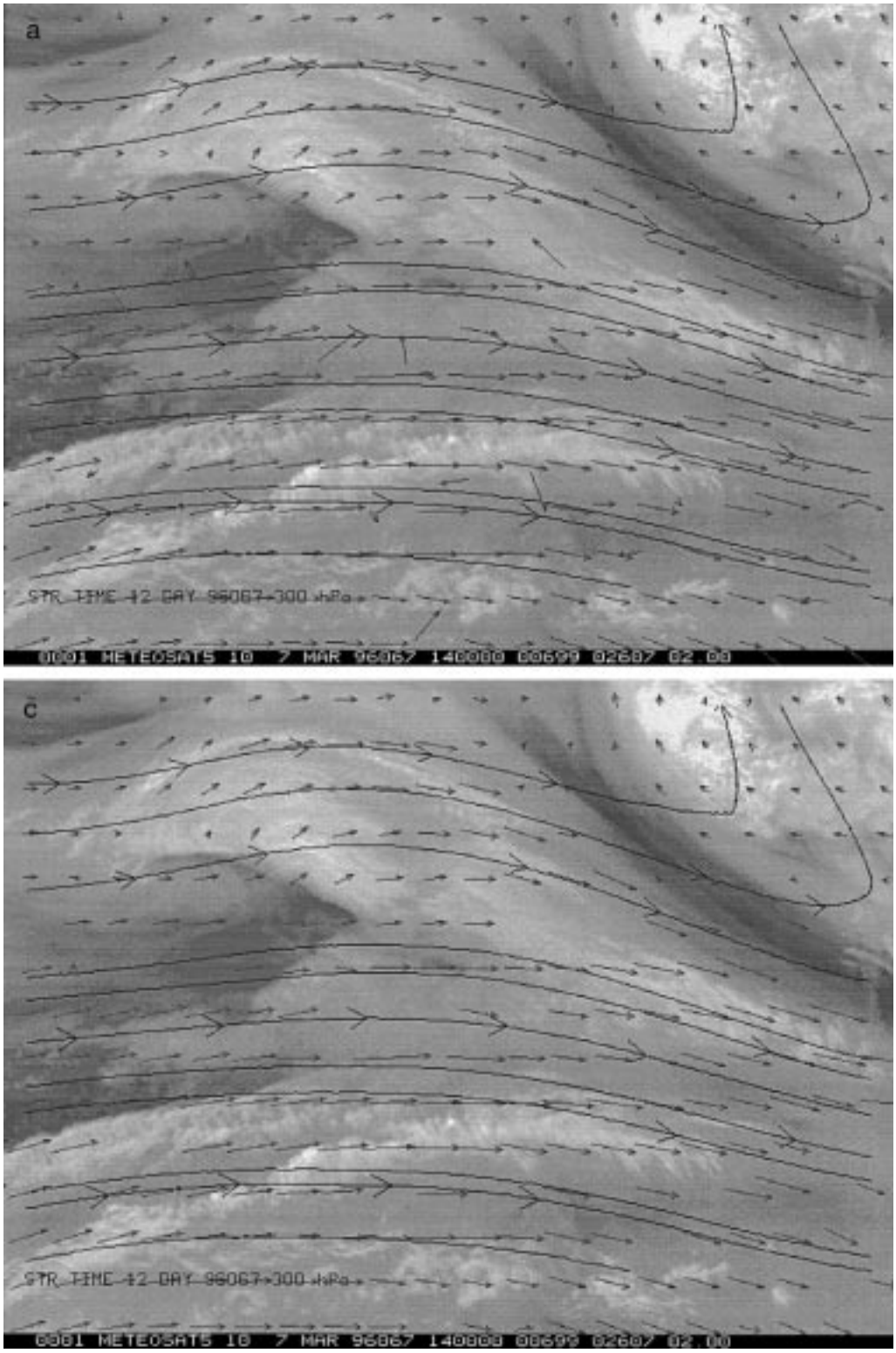

FIG. 3. The impact of different AQC threshold levels for acceptance of WVWVs at 1200 UTC March 7 1997. The pictures, produced with McIDAS (Suomi et al. 1983) show the derived WVWVs (vectors) together with the actual ECMWF 300-hPa analysis field (streamlines) overlaid on the corresponding WV image.

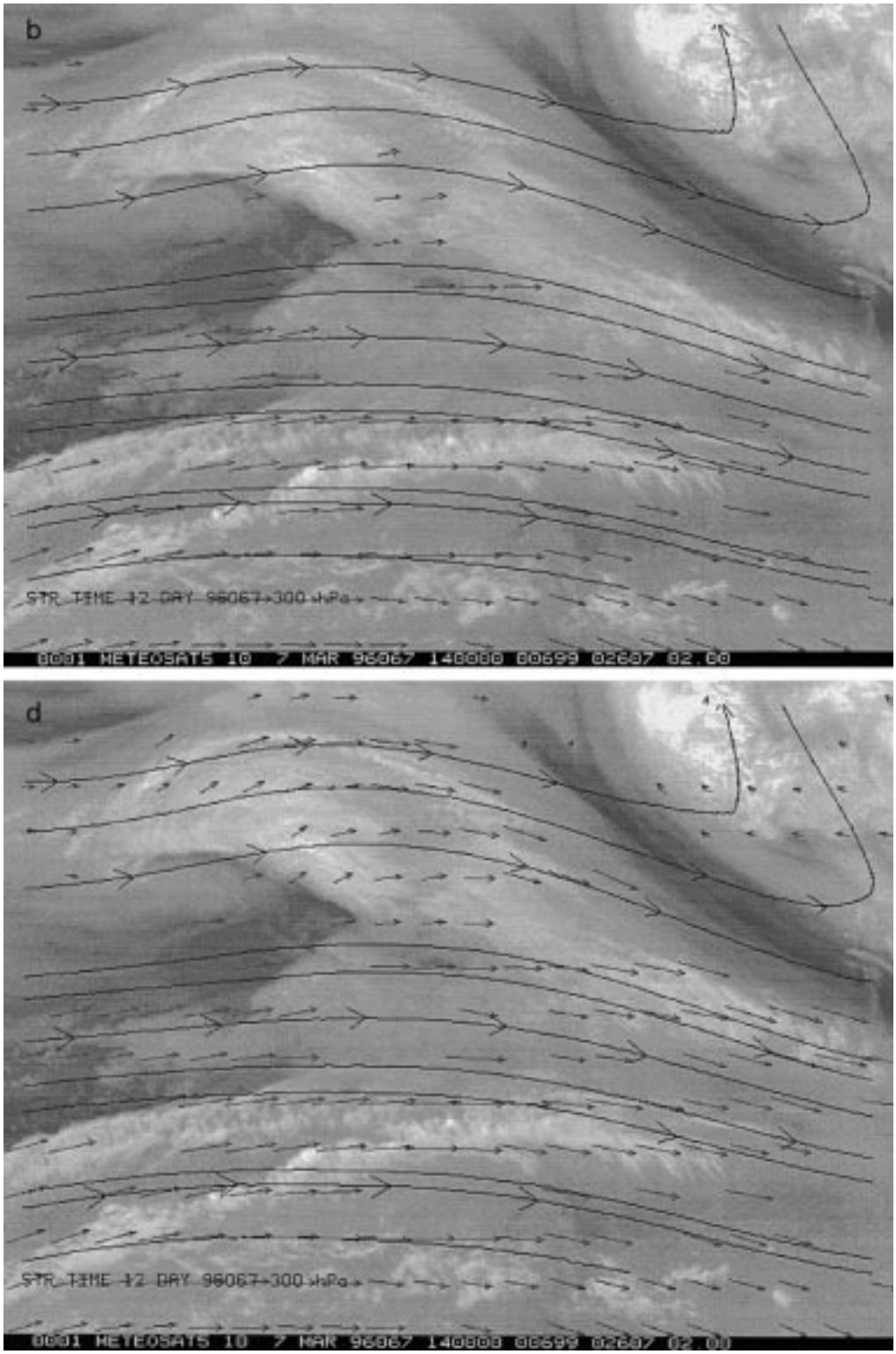

FIG. 3. (*Continued*) The top left shows all derived vectors and the top right the vectors accepted by the traditional AQC. The bottom left shows the vectors with a QI above 0.2 and the bottom right the vectors with a QI above 0.7.

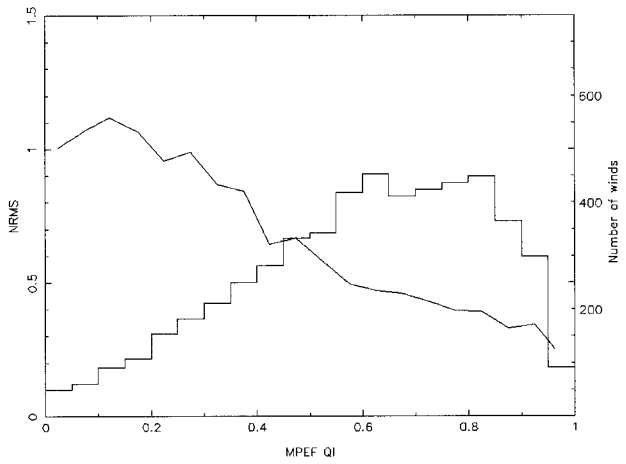

FIG. 4. Nrms vs the MPEF QI for high-level WVWVs in June 1996.

$B/|vec_{R/S}(2)|$]. Therefore the error in the Nrms is introduced through neglecting the variation in $B/|vec|_{R/S}$. For high-level winds the relative error in comparing two periods with each other is then for typical values of rms (8 m s^{-1}), mean wind speed (25 m s^{-1}), and B (1.0) of the order of 10% of the Nrms. For tuning and monitoring purposes we have chosen to use the Nrms as a quick and simple tool to analyze the relative quality of the derived wind vectors. This technique can be applied to periods where no changes are made to the derivation scheme and also when comparing consecutive periods with similar mean wind speeds. Even though the Nrms is not an accurate measure of the true reliability of the winds, problems in the processing scheme are more easily detected with the Nrms than the pure rms value. To validate the derived QI values comparisons against collocated radiosonde measurements were performed. Figure 4 presents the relationship between the Meteorological Products Extraction Facility at Eumetsat (MPEF) reliability estimate against the Nrms for high-level water vapor (WV) winds in October 1996.

The data presented in Figure 4 are based on roughly 5400 R/S measurements collocated with MPEF WVWVs. The collocation data has been sorted according to the MPEF QI into 0.05-wide bins. For each bin the rms vector difference and the mean R/S speed, as well as the mean QI, have been computed. The derived rms and mean R/S speed have then been used to compute the Nrms. The derived Nrms decreases with a simultaneous increase in QI, indicating that the QI contains real quality information. Figure 4 also presents the total number of winds in each bin. In this dataset, 38% of the collocations have a QI above 0.7, which is the current operational automatic cutoff level. This cutoff level accepts more vectors than the traditional AQC, but with an average Nrms similar to the traditional AQC approach, and was therefore selected as the initial threshold to accept vectors. Due to the capability of the new assimilation schemes to digest data with variable quality by adjusting the observation operator according to the characteristics of the observations, it can be expected that the total number of useful vectors can be much higher. For the dataset in question, 88% of the winds have a QI above 0.3.

For medium- and low-level winds the number of collocations is too small to give reasonable results. The rms vector difference for the operationally disseminated vectors, which mainly consist of vectors with a QI above 0.7, is roughly 9 m s^{-1} for a mean wind speed of 24 m s^{-1}. The relationship between the Nrms and the QI shows that it is possible to divide these vectors into groups of different quality. The vectors with the highest mean quality have an Nrms of roughly 0.25, which for a mean wind speed of 24 m s^{-1} is equivalent to an rms vector difference of 6 m s^{-1}. Schmetz et al. (1993) estimated the true error (σ^2_{cmw}) of the upper-level cloud motion winds with

$$\sigma^2_{cmw} = \sigma^2_{cmw,R/S} - \sigma^2_t - \sigma^2_d, \quad (9)$$

where $\sigma^2_{cmw,R/S}$ is the rms vector difference between radiosonde and AMV, and σ^2_t and σ^2_d are the vector differences associated with the separation in horizontal space and time, respectively. For high-level winds Schmetz et al. (1993) used the values 6–7 m s^{-1} for σ_t and 4 m s^{-1} for σ_d, which were based on work by Kitchen (1989), to show that the disseminated wind vectors were of a similar quality to the R/S measurements.

In the current, more detailed approach, a similar estimation of the true error for the different classes is not possible. Applying the above values for σ_t and σ_d together with the above estimation of the rms error in (9) would indicate that the rms error (σ^2_{cmw}) attributed only to the AMVs with a QI above 0.9 is close to zero. The values for σ^2_t and σ^2_d seem, however, too high and may be a result of neglecting speed dependency in the estimates of σ^2_t and σ^2_d. A further problem is that the true relationship between speed and rms vector difference is, as observed by Velden et al. (1997), not quite linear. It is therefore important to investigate the relationship between the QIs and the Nrms also for the winds derived at low and medium levels, for which the speed distribution is different. As the number of collocations for these winds is too small, a comparison against the ECMWF first-guess field was performed.

c. Validation of the QI against the ECMWF first-guess field

The first QI schemes were successfully validated against the ECMWF first guess already in 1994 (CGMS XXIII 1995), but it is only the new four-dimensional variational assimilation schemes (e.g. Tsuyuki 1996; Thépaut et al. 1994) that can fully utilize the QIs. It is therefore important to validate the QIs in the NWP environment as well and, furthermore, to confirm the relationship between the QIs and the quality of the vectors

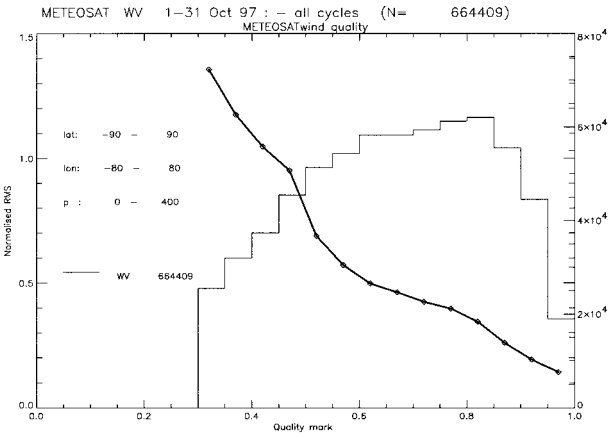

FIG. 5. MPEF QI vs ECMWF Nrms for high-level water vapor wind vectors in October 1997.

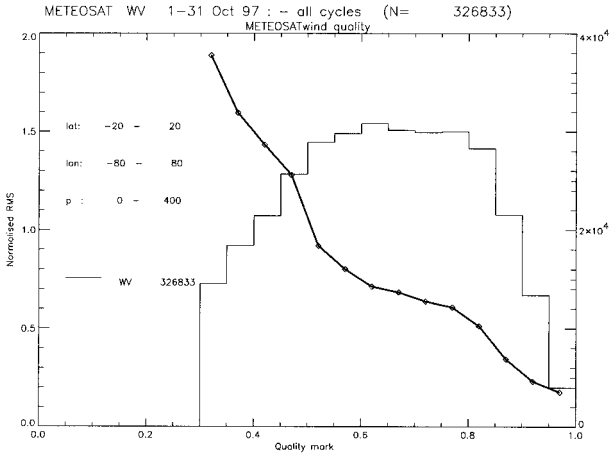

FIG. 7. MPEF QI vs ECMWF Nrms for high-level WVWVs in the Tropics.

derived by the limited radiosonde statistics. This relationship can then be utilized during assimilation to give an appropriate weight to each individual vector, hence maximizing the use of the data.

Since May 1997 EUMETSAT has been disseminating AMVs with a QI greater than 0.3 to ECMWF together with the QI itself. The threshold 0.3 is based on the results derived from statistics against R/S and visual validation of the derived fields. Most vectors with a QI below 0.3 are related to spurious peaks in the correlation surface, hence providing no real information on the local atmospheric conditions. In addition to the standard products derived four times per day, intermediate products (16 per day) are also disseminated. The data are passively monitored in the ECMWF assimilation scheme; that is, it is possible to derive statistics against the model first guess without these vectors impacting the analysis. Figure 5 presents the relationship between the MPEF QI and the Nrms derived from the ECMWF analysis for high-level WVWVs for October 1997 and is based on more than 660 000 disseminated vectors. The data in Fig. 5 are sorted into bins, for which the mean values are derived (in the same way as in Fig. 4). Figures 4 and 5 also show the total number of vectors in the different QI classes.

The results presented for the high-level WVWVs are smoother than the statistics derived against collocated radiosondes. It is important to notice that the highest quality bin (0.95–1.0) has an Nrms of 0.15 and the lowest (0.30–0.35), 1.35. These values are quite different from the values for the collocated radiosondes (0.25 and 0.9, respectively). Figures 6, 7, and 8 present the forecast statistics divided into three latitude bands: Northern Hemisphere (20° to 90°), Tropics (−20° to 20°), and Southern Hemisphere (−90° to −20°).

The results for the Northern Hemisphere region are quite similar to the radiosonde statistics, which are also dominated by the Northern Hemisphere. Therefore the NRMS versus QI relationship should be based on these sets of statistics.

The result for the Southern Hemisphere is similar to

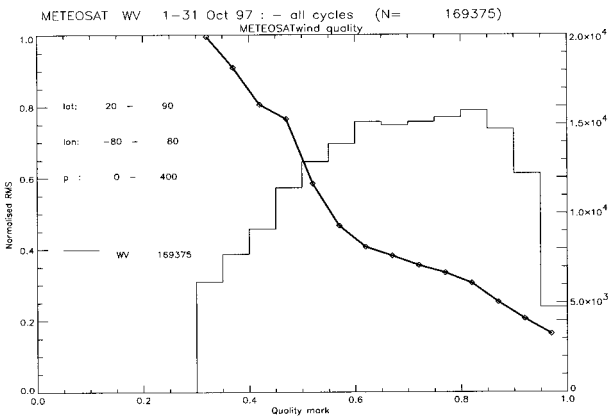

FIG. 6. MPEF QI vs ECMWF Nrms for high-level WVWVs in the Northern Hemisphere.

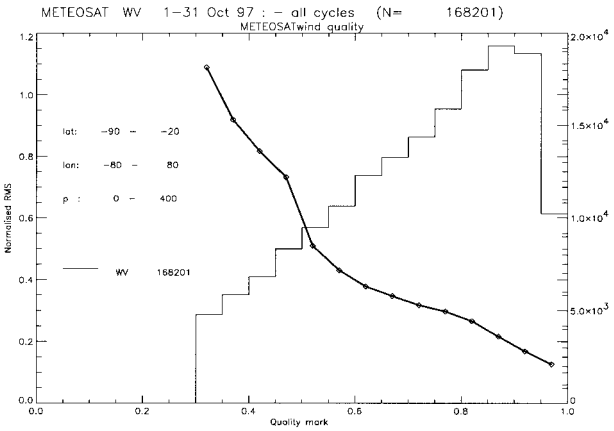

FIG. 8. MPEF QI vs ECMWF Nrms for high-level WVWVs in the Southern Hemisphere.

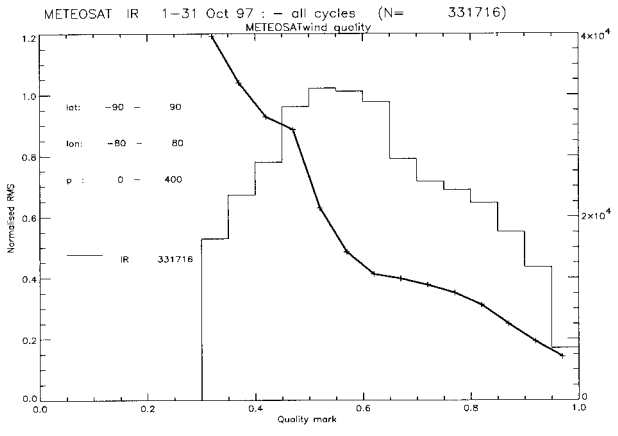

FIG. 9. MPEF QI vs ECMWF Nrms for high-level IR winds in October 1997.

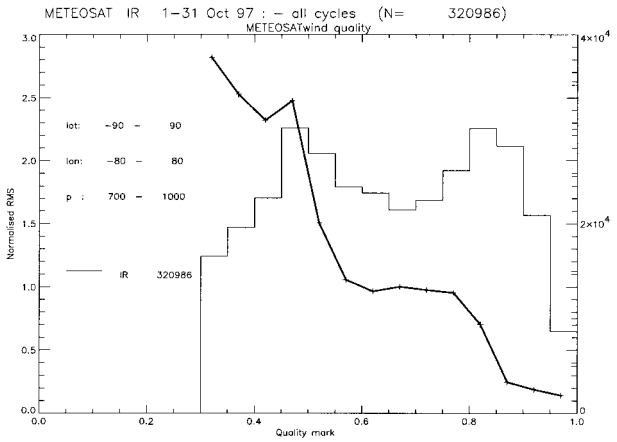

FIG. 11. MPEF QI vs ECMWF Nrms for low-level IR winds in October 1997.

the Northern Hemisphere result, but in the tropical region, which contains roughly 50% of the total amount of vectors, the QI versus NRMS relationship is quite different. This implies differences in the upper-tropospheric flow depicted by the WVWVs as compared to the model field. In the tropical region the relationship between the mass field and wind is not well defined, and as the upper-air measurements are also limited, it is likely that the NWP background field is not of the same quality as in the Northern Hemisphere. This region is also dominated by the ITCZ, with convective clouds, and the derived vectors could therefore represent the dynamic development of the convective clouds rather than represent the prevailing flow. The period under investigation contains only about 420 collocated WVWVs and R/S measurements, and hence dividing the data into similar bins as above is not reasonable. However, the Nrms for all winds with a QI greater than 0.7 is 0.44 (202 collocations), and with QI less than 0.4 (57 collocations) the Nrms is 1.16. These values are higher than the values of the global statistics (0.38 and 0.97, respectively), indicating that the derived vectors are slightly inferior in the tropical region but not as poor as indicated by the ECMWF statistics.

Figures 9, 10, and 11 show the statistics for IR winds derived at different pressure ranges (low = 1000–700 hPa, medium = 700–400 hPa, high = 400–100 hPa). Figure 12 shows the comparison for winds derived by using data from the visible channel.

The results for the high-level IR winds are similar to the high-level WVWVs, with a monotonic increase in quality with a simultaneous decrease in Nrms. For the medium level the results are poor. Most vectors have a quality below 0.6, and furthermore the relationship between QI and NRMS is not well defined. This is, however, not related to the derivation of the QIs, but is more an indication of problems in the derivation of medium-level winds and their height assignment.

The low-level IR winds also show a similar lack of information in the QI region around 0.6. The reason for this is mainly due to discrepancies in height assignment, especially in the vicinity of the boundary layer, where

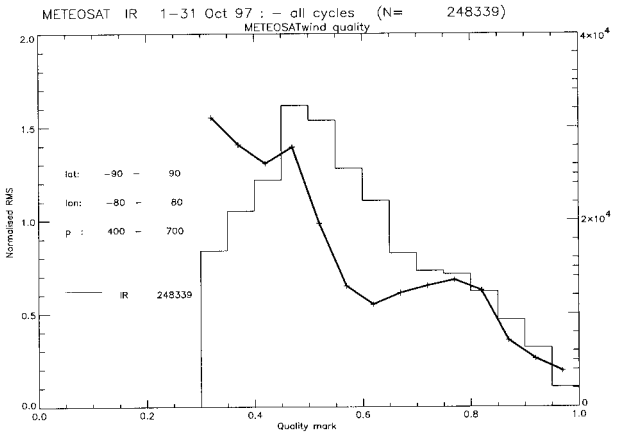

FIG. 10. MPEF QI vs ECMWF Nrms for medium-level IR winds in October 1997.

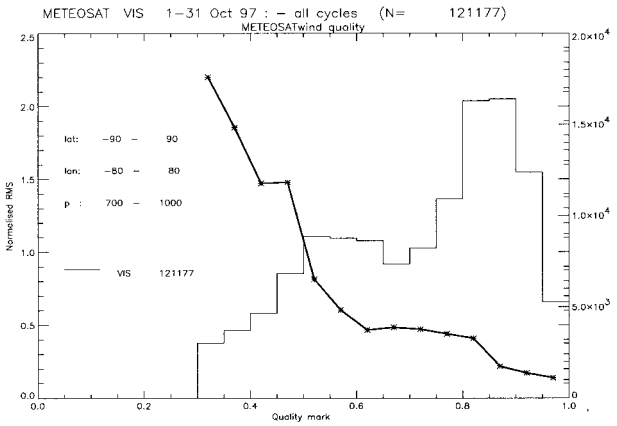

FIG. 12. MPEF QI vs ECMWF Nrms for low-level visible winds in October 1997.

a small error in the assigned height or depth of the boundary layer in the model can result in large vector differences due to strong wind shear. A further problem is very thin high-level cirrus, which might remain undetected in the cloud analysis and is falsely assigned to low levels but still provides enough information for the correlation procedure to identify the high-level motion (Ottenbacher et al. 1997). In these cases the tracking and height assignment can be consistent, providing relatively high QIs. The latter problem is also visible in the statistic for the low-level visible winds (Fig. 12).

Generally the behavior of the Nrms against the MPEF QI for the visible winds is good; however, the relationship is not as clear as for high-level winds. A close look at some individual results has shown that this is a result of the thin cirrus cloud problem mentioned above. These poor vectors can be identified with an interchannel consistency check (Holmlund 1997). This new test compares the extracted low-level winds against collocated high-level WVWVs. Vectors with a high degree of agreement are most likely not representative of the low-level flow and should therefore be removed. This test will be included in the operational scheme in late 1997 or early 1998. Finally it should be noted that the distribution of the visible winds are dominated by winds with a high QI as opposed to the IR low-level winds. For the latter there are roughly the same amount of winds with a quality around 0.5 and 0.8–0.9.

4. Future developments

The current AQC approach displays some areas where further improvements can be foreseen. The highest success of the QIs is demonstrated for high-level WVWVs. This clearly reflects the tuning of the scheme, which has, to a large extent, been based on these vectors. The results have then been applied to vector fields derived with other channels and at other levels.

Despite the successful implementation of the current scheme to low-level visible winds, there is a potential to improve the system for vector fields derived from data of the other Meteosat channels and for other levels. The introduction of an interchannel consistency check is expected to improve the results, especially for the low-level winds.

The full utilization of the QIs also needs further validation. It is foreseen that as a next step in the validation process, ECMWF will use wind fields derived at a higher frequency than is currently used and exploit the QIs in the four-dimensional assimilation process. The final assessment will be performed with model impact studies.

The current methodology has only been thoroughly validated for the final QI. The use of the tanh-based function to normalize the quality tests is adequate, especially for high-level winds. To fully utilize the capabilities of the AMVs the QI should be split up into individual components: speed, direction, and height, where the estimation of the reliability of the height assignment poses the greatest challenge. This implies further investigations and tuning of the individual tests and of associated weights.

5. Conclusions

A new method to derive quality information of individual wind vectors derived from consecutive satellite imagery has been presented. The subjective analysis, as well as the objective validation performed against R/S data and ECMWF analysis, shows that the derived quality indicators (QIs) can be used to identify good quality vectors. The derived statistics show that the normalized rms (Nrms) difference between the derived atmospheric motion vectors and the R/S as well as ECMWF first-guess winds decreases monotonically with increase in the estimated quality. The R/S comparisons show that wind vectors with a QI above 0.9 have an Nrms of 0.3, whereas the winds with a QI below 0.4 have an Nrms of 0.6 or higher. These Nrms values are for a mean wind speed of 20 m s^{-1} equivalent to a vector rms of 6 m s^{-1} and 12 m s^{-1}, respectively. The results derived against the ECMWF first guess are quite similar for the Northern Hemisphere. The relationship between Nrms and QI is, however, more pronounced. The vectors with a QI above 0.9 have an Nrms of 0.2, whereas the Nrms for the vectors with a QI below 0.4 is above 0.8.

The derived QIs are currently being disseminated together with the individual wind vectors to ECMWF for monitoring. It is expected that the QIs will become fully operational during 1997 and will enable more effective assimilation of the products, providing an enhanced utilization of atmospheric motion vectors derived from satellite imagery.

As a result of the positive experience with the AQC scheme, EUMETSAT has, as of 7 September 1998, abandoned manual quality control of individual vectors.

Acknowledgments. Thanks are due to shift meteorologists J. Gustafsson and M. Lindberg for validating the new scheme, to Dr. Michael Rohn for the ECMWF collocations, to the three reviewers for their feedback that helped to improve the paper, and to Dr. Chris Velden for his constructive comments.

REFERENCES

Berz, G., 1983: Verteilungen. *PROMET,* Vol. 1, 11–16. [Available from German Weatherservice, Frankfurter Strasse 135, 6050 Offenbach, Germany.]

Bhatia, R. C., P. N. Khanna, and S. Prasad, 1996: Improvements in automated cloud motion vectors (CMWs) derivation scheme using INSAT VHRR data. *Proc. Third Int. Winds Workshop,* Ascona, Switzerland, EUMETSAT, 37–43.

Buhler, Y., and K. Holmlund, 1994: The CMW extraction algorithm for MTP/MPEF. *Proc. Second Int. Wind Workshop,* Tokyo, Japan, EUMETSAT, 205–218.

CGMS XXIII, 1995: Report of the Twenty-third Meeting of the Coordination Group for Meteorological Satellites. 54 pp. plus ap-

pendixes. [Available from EUMETSAT, Am Kavalleriesand 31, 64295 Darmstadt, Germany.]
DeGaetano, A. T., 1997: A quality control routine for hourly wind observations. *J. Atmos. Oceanic Technol.,* **14,** 308–317.
Endlich, R. M., and G. S. McLean, 1957: The structure of the jet stream core. *J. Meteor.,* **14,** 543–552.
Hayden, C., and C. Velden, 1991: Quality control and assimilation experiments with satellite derived wind estimates. Preprints, *Ninth Conf. on Numerical Weather Prediction,* Denver, CO, Amer. Meteor. Soc., 19–23.
——, and R. J. Purser, 1995: Recursive filter objective analysis of meteorological fields, applications to NESDIS operational processing. *J. Appl. Meteor.,* **34,** 3–15.
Holmlund, K., 1994: Operational water vapour wind vectors from Meteosat imagery data. MPEF. *Proc. Second Int. Wind Workshop,* Tokyo, Japan, EUMETSAT, 77–84.
——, 1995: Half hourly wind data from satellite derived water vapour measurements. *Adv. Space Res.,* **16,** 1059–1068.
——, 1997: Quality indicators for atmospheric motion vectors: Reliability and impact on the EUMETSAT product generation. *Proc. 1997 Meteorological Satellite Data Users Conference,* Brussels, Belgium, EUMETSAT, 355–362.
Holton, J. R., 1979: *An Introduction to Dynamic Meteorology.* 2d ed. Academic Press, 391 pp.
Kelly, G., 1993: Numerical experiments using cloud motion winds at ECMWF. *Proc. Developments in the Use of Satellite Data in Numerical Weather Prediction,* Reading, United Kingdom, ECMWF, 331–348.
Kitchen, M., 1989: Representativeness errors for radiosonde observations. *Quart. J. Roy. Meteor. Soc.,* **115,** 673–700.
Le Marshall, J., N. Pescod, B. Seaman, G. Mills, and P. Stewart, 1994: An operational system for generating cloud drift winds in the Australian region and their impact on numerical weather prediction. *Wea. Forecasting,* **9,** 361–370.
Menzel, P., C. M. Hayden, S. J. Nieman, C. S. Velden, and S. Wanzong, 1996: Improvements in the quality assessment of automated satellite-derived cloud and water vapour motion vectors. *Proc. Third Int. Winds Workshop,* Ascona, Switzerland, EUMETSAT, 197–205.
Nieman, S., W. P. Menzel, C. M. Hayden, D. D. Gray, S. Wanzong, C. Velden, and J. Daniels, 1997: Fully automated cloud-drift winds in NESDIS operations. *Bull. Amer. Meteor. Soc.,* **78,** 1121–1133.
Nuret, M., 1990: Production operationelle de vecteurs de placement de nuage a partir de l'image de Meteosat. *Meteorologie,* **31,** 7–16.
Ottenbacher, A., M. Tomassini, K. Holmlund, and J. Schmetz, 1997: Low-level cloud motion winds from Meteosat high-resolution visible imagery. *Wea. Forecasting,* **12,** 175–184.
Prater, E. T., 1996: Aircraft measurements of ageostrophic winds. *J. Appl. Meteor.,* **35,** 2040–2056.
Rattenborg, M., and K. Holmlund, 1996: Operational wind products from new Meteosat ground segment. *Proc. Third Int. Winds Workshop,* Ascona, Switzerland, EUMETSAT, 53–59.
Schmetz, J., K. Holmlund, J. Hoffman, B. Strauss, B. Mason, V. Gärtner, A. Koch, and L. van de Berg, 1993: Operational cloud-motion winds from Meteosat infrared images. *J. Appl. Meteor.,* **32,** 1206–1225.
Suomi, V. E., R. J. Fox, S. S. Limaye, and W. L. Smith, 1983: McIDAS III: A modern interactive data access and analysis system. *J. Climate Appl. Meteor.,* **22,** 766–778.
Tenenbaum, J., 1996: Jet stream winds: Comparisons of aircraft observations with analysis. *Wea. Forecasting,* **11,** 188–197.
Thépaut, J.-N., R. N. Hoffman, and P. Courtier, 1993: Interactions of dynamics and observations in a four-dimensional variational assimilation. *Mon. Wea. Rev.,* **121,** 3393–3414.
Thoss, A., 1992: Cloud motion winds, validation and impact on numerical weather forecast. *Proc. First Int. Wind Workshop,* Washington, DC, EUMETSAT, 105–112.
Tokuno, M., 1996: Operational system for extracting cloud motion and water vapour motion winds from GMS-5 image data. *Proc. Third Int. Winds Workshop,* Ascona, Switzerland, EUMETSAT, 21–30.
Tsuyuki, T., 1996: Variational data assimilation in the Tropics using precipitation data. Part II: 3D model. *Mon. Wea. Rev.,* **124,** 2545–2561.
Velden, C., 1996: Positive impact of satellite-derived winds during the 1995 hurricane season: Example of optimizing data application and processing strategy. *Proc. Third Int. Winds Workshop,* Ascona, Switzerland, EUMETSAT, 81–89.
——, C. M. Hayden, W. P. Menzel, J. L. Franklin, and J. Lynch, 1992: The impact of satellite-derived winds on numerical hurricane track forecasting. *Wea. Forecasting,* **7,** 107–118.
——, ——, M. S. J. Nieman, W. P. Menzel, S. Wanzong, and J. S. Goers, 1997: Upper-tropospheric winds derived from geostationary satellite water vapor observations. *Bull. Amer. Meteor. Soc.,* **78,** 173–195.
——, T. L. Olander, and S. Wanzong, 1998: The impact of multispectral *GOES-8* wind information on Atlantic tropical cyclone track forecasts in 1995. Part I: Dataset methodology, description, and case analysis. *Mon. Wea. Rev.,* **126,** 1202–1218.